Volume 7, Issue 3, 2026

Trends in
Natural Products Research

Isolation and Characterization of Bioactive Compounds in S*enna siamea* Leaf and their Inhibitory Activity Against *Salmonella gallinarum* and *Salmonella pullorum*

Matthew Egbono Otor *[1,2], Timothy Akpomie[1], Abdullahi Usman[1]

[1]Department of Chemistry, Federal University of Lafia
[2]Biochemistry Division, National Veterinary Research Institute, Vom

Abstract

Senna siamea is known for its medicinal properties, including antimicrobial activity. With increasing antibiotic residue in meat and egg, there is a need to search for alternative treatment for fowl typhoid and pullorum disease. This work aimed to isolate and characterize bioactive compounds in *Senna siamea* leaves with inhibitory activity against *S. gallinarum* and *S. pullorum*. Ethanol extract was subjected to liquid-liquid extraction with chloroform, ethyl acetate, and butanol. Column chromatography analysis of the ethyl acetate fraction of ethanol extract gave two pure compounds with molecular weights of 870.5886 Da and 412.3705 Da, by mass spectrometer. Nuclear magnetic resonance data, such as 1H NMR, 13C NMR, COSY, HSQC, and HMBC, and mass spectrometer resolution revealed the two compounds as pheophytin A and stigmasterol, respectively Against *S. gallinarum* and *S. pullorum*, pheophytin A had an inhibitory zone of 23 mm while stigmasterol had an inhibitory zone of 22 mm at 100 µg/mL. The MICs for the two compounds was 25 µg/mL. The minimum concentration required to kill the bacteria is 25 µg/mL for pheophytin A and 100 µg/mL for stigmasterol. Molecular docking yielded a positive result with stigmasterol, while pheophytin A could not be docked because of its high molecular weight. Swiss ADME was used to predict adsorption, distribution, metabolism, excretion, and toxicity, while Protox 3 was used to predict the toxicity profile of the compounds. Pheophytin A has an LD_{50} of 40 mg/kg, and stigmasterol has an LD_{50} of 890 mg/kg. The toxicity profile revealed that there was no hepatotoxicity, carcinogenicity, mutagenicity, or cytotoxicity for the two compounds. Pheophytin A is not soluble, while stigmasterol is moderately soluble in water.

Keywords: Salmonella, *Senna siamea*, stigmasterol, pheophytin A, toxicity

*Corresponding author:
otormatty@yahoo.com
+234 8134709120
https://doi.org/10.61594/tnpr.v7i3.2026.171
Page No.: 239-251
Volume: Volume 7 Issue 3, 2026
Trends in Natural Products Research

Introduction

The global demand for meat and egg has increased substantially over recent decades, driven by rising income levels, rapid urbanization, and sustained population growth (Zhou *et al*., 2022). Among livestock enterprises, poultry production represents one of the fastest-growing sector, owing to its ability to supply high-quality animal protein, its relatively short production cycle, and superior feed conversion efficiency when compared with other livestock species (Marangoni *et al*., 2015) . These advantages have positioned poultry as a critical component of global food security.

Despite this growth, infectious diseases remain a major limitation to sustainable poultry production, with avian salmonellosis constituting one of the most economically significant challenges (Shivaprasad, 2000). The disease is increasingly recognized as a multidrug-resistant condition that poses serious threats to poultry health and productivity (Ziaul *et al*., 2021). Members of the genus Salmonella are rod-shaped, Gram-negative bacteria classified into Salmonella enterica and *Salmonella bongori*, with *S. enterica* subsp. enterica, comprising over 1,400 serovars. Among these, *Salmonella gallinarum* and *Salmonella pullorum* are host-adapted pathogens responsible for fowl typhoid and pullorum disease, respectively, both of which cause severe morbidity and mortality in poultry populations (Berhanu, 2020). Conventional management of these diseases relies heavily on antibiotic therapy.

However, the extensive and often indiscriminate use of antibiotics in poultry production has raised significant public health concerns, particularly regarding the persistence of antibiotic residues in poultry meat and eggs. Chronic exposure to such residues through the food chain can accelerate the emergence and dissemination of antibiotic-resistant bacteria, thereby reducing the effectiveness of existing antimicrobial agents. Furthermore, the transfer of resistant bacterial strains from animals to humans represents a growing global health risk (FAO, 2016).

In response to these challenges, medicinal plants have attracted considerable scientific interest as alternative sources of antimicrobial agents. Plant-derived bioactive compounds possess structural diversity and are capable of interacting with microbial pathogens through multiple mechanisms of action, in contrast to most conventional antibiotics that typically target a single cellular site (Nützmann *et al*., 2016). This multi-target activity is considered advantageous in mitigating the development of antimicrobial resistance.

Senna siamea (Lam.) H.S. Irwin & Barneby, commonly known as kassod tree or yellow cassia, is a medicinal plant introduced into Africa from tropical Asia and is now widely cultivated throughout tropical regions of the continent. Various parts of the plant—including the leaves, stems, roots, flowers, and seeds—have been traditionally employed in the treatment of several ailments, with the leaves being the most frequently used component in herbal preparations among African and Asian populations (Nas *et al*., 2018). Ethnomedicinal applications of *S. siamea* include the management of malaria, constipation, diabetes, insomnia, hypertension, asthma, typhoid fever, and diuretic disorders (Nas *et al*., 2018).

Several *in vitro* studies (Abdulrasheed *et al*., 2015; Nas *et al*., 2018) have demonstrated the antibacterial potential of *S. siamea* leaves. It was reported that both crude extracts and solvent fractions of leaves exhibited significant inhibitory activity against *Salmonella gallinarum* and *Salmonella pullorum* (Otor *et al*., 2025). Despite these findings, there remains limited information on the specific bioactive compounds responsible for this anti-salmonella activity.

Therefore, the present study aimed to isolate and characterize the bioactive compounds in *Senna siamea* leaves and test their inhibitory activity against *Salmonella gallinarum* and *Salmonella pullorum*, with the ultimate goal of providing a scientific basis for the development of plant-based antimicrobial agents for fowl typhoid and pullorum diseases.

Materials and methods

Plant collection and identification

Senna siamea leaves were harvested in March 2024 from their natural habitat in the National Veterinary Research Institute, Vom, Plateau State, Nigeria (Latitude 9.7300 ° N and longitude 8.7874 ° E). The plant was identified by Mr. O.E Agyeno at the Herbarium of the Department of Plant Science and Biotechnology, Faculty of Natural Sciences, University of Jos, Plateau State, Nigeria, where a voucher specimen number JUHN23000627 was assigned.

Drying and pulverization of plant material

Senna siamea leaves were rinsed in clean water and dried at room temperature.The dried leaves were pulverized using a wooden mortar and pestle and stored in a clean polythene bag (Lisa 2023).

Extraction of plant material

Powdered *Senna siamea* leaves (1 kg) were macerated in 1.5 L of 100% petroleum ether at room temperature for 48 h. The extract was filtered, and the marc (residue) was dried. A 500 g of the marc was extracted by maceration in 1 L of absolute ethanol at room temperature for 48 h. The extract was filtered through a 150 µm sieve, then re-filtered through Whatman No.1 filter paper (Lisa Nichols, 2023)

Fractionation (liquid-liquid extraction)

The ethanol extract was subjected to fractionation by liquid-liquid extraction. A 50 g of ethanol extract was reconstituted

in 200 mL distilled water in a 1000 mL conical flask and covered with a stopper and allowed to dissolve properly by agitation. This was poured into a separating funnel. Three solvents chloroform, ethyl acetate and butanol were selected for the separation. Chloroform (100 ml) was poured into the reconstituted extract in the separation funnel and agitated for 3 minutes. This was allowed to separate into two phases, the lower layer containing chloroform and its bioactive compounds and upper layer contained the aqueous layer. The chloroform layer was collected into a container while the aqueous portion was collected into another volumetric flask. The aqueous portion was returned into the separatory funnel and the cycle continued until a clear chloroform layer was seen below the aqueous phase.

The same process was carried out for both ethyl acetate and butanol. The micelles from ethyl acetate and butanol obtained from the partitioning were air dried while the aqueous portion was oven dry at 50ºC (Otor *et al*., 2025).

Column chromatography

Silica gel was used as the stationary phase in a chromatography column, which was prepared using the wet method. The column (80x3cm) was packed with 70 g of silica gel mixed with hexane to create a slurry, which was carefully poured into the column. After allowing the hexane to settle, 2 g of the ethyl acetate fraction was introduced. A series of hexane and ethyl acetate mixtures (90:10-10:90) was used to separate the fraction, with 20 ml aliquots collected in vials until a total of 110 vials were collected (Lisa, 2021). Fractions with similar R_f values were merged. All fractions were coded as MPH

Spectroscopic Analysis

Proton (^{1}H) and ^{13}C Nuclear Magnetic Resonance (NMR) Spectra were acquired on a Bruker AV-3 (400 MHz) Spectrophotometer using $CDCl_3$. The Mass Spectra were acquired using an Agilent 6130 mass spectrometer. The spectra were processed using Mestre Nova software, and the data were interpreted to obtain the actual structures of the compounds isolated. The isolated compounds were screened for antimicrobial activity.

Antimicrobial screening of the isolated compounds

Isolates of *Salmonella gallinarum* and *Salmonella pullorum* were obtained from Microbiology Laboratory of Central Diagnostic National Veterinary Research Institute Vom, Plateau State, Nigeria. The anti-*Salmonella* (*gallinarum* and *pullorum*) activity of the isolated compounds was determined using the agar well diffusion method. A freshly prepared broth was poured into a petri dish and allowed to solidify at room temperature. The plates were incubated at 37°C for 24 h before being used, to ensure that there is no contamination of the plates. Aliquot (1 mL) of the already prepared isolate was inoculated into the broth by evenly distributing it by gentle swirling of the plate. Three wells were made on the broth in the plates. The wells were filled with about 1 mL of the isolated compounds (25, 50, and 100 µg/mL). Dimethyl sulfoxide (DMSO) was used as a control since it was used as a solvent. The petri dish was incubated at 37°C for 24 h. After which, the antimicrobial activity of the isolated compounds was obtained by measuring the zone of inhibition.

Determination of minimum inhibitory concentration (MIC) and minimum bactericidal concentration (MBC) of the isolated compounds

The MIC and MBC were determined by preparing three concentrations of the isolated compounds. 100 µg/mL concentration was prepared, and two other concentrations; 50 and 25 µg/mL, were prepared by serial dilution in test tubes. A loopful of isolate of the bacteria was inoculated into the compound in the test tube and incubated at 37°C for 24 h. The test tubes were observed for turbidity at different concentrations for MIC. MBC was determined by re-culturing the inoculum from each of the test tubes in a petri dish containing the broth and incubated at 37°C for 24 h. The plates were observed for growth, and the MBC was recorded as the least concentration of extract in which there was no growth of the bacteria (Otor *et al*., 2025).

Molecular Docking (In silico) studies

The molecular docking was carried out on the isolated compounds from the ethyl acetate fraction using Schrodinger, a docking software.

Results

Compounds characterization

Characterization of MPH-12 as pheophytin A

This fraction was isolated as dark green powder. The HR–LCMS detected a dominant molecular ion at m/z 871.5886 (calculated 871.5732) corresponding to the protonated molecule [M + H] in positive mode HR–LCMS, which is consistent with the molecular formula $C_{55}H_{74}N_4O_5$ and molecular weight of 870.5886 Da for the neutral molecule of pheophytin A. The ^{1}H NMR spectrum data (Table 1) revealed singlet signals which were observed at 9.49, 9.35, and 8. 54 corresponding to H-10, H-5, and H-20, characteristics of olefinic methinic proton of the porphyrin unit. Other signals observed were 3.66 (s, methyl, H-12^1), 3.38 (s, methyl, H-2^1), 3.19 (s, methyl-7^1), 1.87 (d, J =7.0 Hz, methyl-18^1) and 1.62 (t, J=7.5 Hz, methyl-8^2) which is made up four methyl groups and one ethyl group appearing as substituents on pyrrole rings of the porphyrin unit. With additional signals such as the triplet at 3.63 ppm (2H-8^1), methoxy group at 3.90 ppm (br s,3H-13^4), and 7.96 ppm [dd, 17.8 and 11.5 Hz,] a double bond substituent linkage to C-3. Signals at 4.22 and 5.22 are characteristic of ester and olefinic protons of the phytyl group.

Downfield resonances between δH 6.16–6.30 ppm were attributed to β-pyrrolic and vinylic protons within the conjugated chlorin core, while upfield methyl and methylene signals between δH 0.55–1.50 ppm corresponded to the long-chain phytyl group.

The ^{13}C NMR spectrum data (Table 1) revealed the presence of several signals. Three Carbonyl groups were observed at 179.57 ppm (C-13^{1}), 162.53 ppm (C-133), and 172.49 ppm (C-17^{3}) as sp^{2,} respectively. An oxygenated sp^{3} hybridized carbon at 61.58 ppm and a methoxy group at 53.38. In addition, other signals were observed at 104.21 ppm, 97.91 ppm, and 93.63 ppm, corresponding to the methinic (=CH) carbons of C-10, C-5, and C-20, indicating a porphyrin moiety. The signals at 51.90 ppm and 50.37 ppm correspond to C-17 and C-18 methine carbons of the porphyrin moiety, while the signal at 61.58 ppm (-COOCH2) corresponds to the oxymethylene carbon. The information above confirmed that MPH-12 is pheophytin a

2D dimension NMR data (COSY, HSQC, HMBC) were studied to establish proton-proton and proton-carbon connectivity. The HSQC spectrum data showed correlations between several carbons and hydrogen atoms including the carbon atom (C-10) at 104.21 ppm and the proton (H-10) at 9.49 ppm, C-5 at 97.91 ppm and H-5 at 8.35 ppm and the carbon atom (C-20) at 93.63 ppm and the proton (H-20) at 9.35 ppm, characteristic of porphyrin moiety of olefinic methine (=CH) groups bonded to pyrrole rings. Single bond coupling were observed between the carbon atom at 12.96 (C-12^{1}) ppm and the protons (H-12^{1}) at 3.66 ppm; C-2^{1} at 12.96 ppm and H-2 at 3.38 ppm; C-7^{1} at 11.6 0 ppm and H-7^{1} at 3.13 ppm; C-18^{1} at 22.70 ppm and H-18^{1} at 1.87 ppm, are characteristic of four methyl and one ethyl substituents attached to the pyrrole rings of the porphyrin unit. In addition, there were also correlations between the carbon atom (C-8^{1}) at 19.50 ppm and the protons (H-8^{1}) at 3.66 ppm; the oxymethyl (COOCH3) carbon (C-13^{4}) at 53.38 ppm and its protons (H-13^{4}) at 3.90 ppm; the olefinic carbons (C-3^{1}) at 129.02 ppm and C-3^{2} at 122.79 ppm and their corresponding protons (H-3^{1}) at 7.96 ppm and (H-3^{2}) at 6.30 ppm, respectively.

The Correlation Spectroscopy (COSY) spectra revealed strong ^{2}J and ^{3}J coupling interactions among aromatic and vinylic protons within the porphyrin at 6.16, 6.27, and 6.30 ppm. These cross-peaks are indicative of linkages between adjacent β-pyrrolic hydrogens (H-3, H-10, and H-20). Cross peaks were also observed at the aliphatic region between 1.20 and 0.55' 0.88 ppm, which showed the connection between CH_2–CH_3 units in the phytyl chain.
Heteronuclear Multiple Bond Correlation (HMBC) spectroscopy, provided long-range (^{2}JCH and ^{3}JCH) correlations that linked protonated and non-protonated carbons across the molecular skeleton. The ester carbonyl at δC 179.57 ppm showed strong three-bond correlations with the O–CH_2 protons at δH 3.3–4.8 ppm, confirming the phytyl–macrocycle linkage. Likewise, the formyl and conjugated carbonyl carbons (δC 162 -172 ppm) exhibited long-range couplings with vinylic and aromatic protons (δH 6.27-6.30 ppm), establishing the positions of electron-withdrawing substituents around the ring. These long-range correlations are fundamental to defining the macrocyclic architecture, bridging quaternary centers that are otherwise invisible in direct proton detection. (Shrivastava and Mishra, 2019).

From the ^{13} Carbon NMR data, a total of 10 sp^{2} (non-protonated) carbons were observed between 179.57- 142.06 ppm by the absence of HSQC correlations. The absence of the remaining 9 of these carbons in this study could be as a result of overlap or degeneracy and low intensity. These correspond to quaternary and carbonyl carbons within the conjugated chlorin macrocycle. With a further 12 sp^{2} protonated carbon (CH) observed between 137.82-107.74, while the other carbons are sp^{3} carbon (CH_2) from 71.83- 24.71 ppm, and methyl groups of the phytyl chain. Among the carbons in this region are O-CH and O-CH2 at 71.83 and 61.58 ppm.
Other observed features are fourteen methylene carbon including a sp^{2} methylene at δC 122.79 ppm, and a sp^{3} oxygenated at 61.58 ppm, were detected.

All the above spectral data in comparison with literatures, (Rodrigues *et al*., 2014), (Friday *et al*., 2021), (Odo *et al*., 2022) were used to build the structure of the isolated compound as pheophytin A as shown in Figure 1

Table 1: NMR experimental data for MPH-12

Position	^{1}H δ ppm	Position	^{13}C δ ppm	Literature Rodriques *et al.,* 2014 ^{1}H δ ppm	^{13}C ppm
H-10	9.49 (s)	C-13^{1}	179.57	9.51	189.83

H-5	9.35 (s)	C-19	172.49	9.35	172.45
H-20	8.54(s)	C-16	162.53	8.56	169.83
H-3[1]	7.96 (dd, *j*=17.85 and 11.48 Hz)	C-6	155.33	7.97	155.83
H-3[2]	6.30(d)	C-9	151.02	6.29	151.19
H-13[2]	6.27(*trans*, d, *j*=17.95 Hz)	C-9/C-14	149.90	-	149.85
H-3[2]	6.15 (cis, d, j=11.10 Hz)	C-8	145.16	6.14	145.49
H-13	5.40 (m)	C-1	142.73	-	142.27
H-2'	5.22 (m)	C-11	137.82	5.15	138.14
H-18	4.51 (m)	C-3/C-4	136.45	4.52	136.38
H-17	4.42 (m)	C-2	131.74	4.42	132.06
	4.25	C-3[1]	129.37	4.25	129.30
H-13[4]	3.90(s)	C-12	129.02	3.90	129.19
H-12[1]	3.70 (s)	C-3²	122.79	3.69	122.96
H-8[1]	3.65 (m)		117.78	3.66	117.94
H-2[1]	3.38 (s)		116.24	3.40	
H-7[1]	3.20 (s)	C-15	107.74	3.21	105.46
H-17[1]	2.64 (m), 2.39 (m)	C-10	104.21	2.64 (m), 2.37 (m)	104.63
H-17[2]	2.52 (m), 2.22 (m)	C-5	97.91	2.50 (m), 2.23 (m)	97.75
H-18[1]	1.87 (d)	C-20	93.63	1.89	93.63
H-8[2]	1.62 (m)	C-13[2]	61.58	1.61	61.67
H-8'	1.20 (m)	C-13[4]	53.38	1.21	53.04
H-17[1]	1.14(d, *j*=7.0 Hz)	C-17	51.90	1.12	51.83
Phytyl CH_3	0.95 (d, *J*=6.8 Hz)	C-18	50.37	-	50.33
Phytyl CH_3	0.88 (t, *J*=7.0 Hz)		39.85	0.86	39.55
Phytyl CH_3	0.72 (d, *J*=6.8 Hz)		37.28	0.81	37.46
Phytyl	0.55 (s)		32.77	-	32.81
		C-17[2]	31.52	-	31.45
		C-17[1]	29.69		30.03
			27.91		28.11
			25.64		25.19
			24.71		24.98
		C-18[1]	22.70		22.91
			22.65		22.81
		C-8[1]	19.96		19.19
		CH3 2[1]	12.98		12.28
		C-7	11.6		11.40

Proton (^{1}H) and carbon (^{13}C) NMR chemical shift data (δ, ppm) of the compound, including signal multiplicities and coupling constants (J, Hz) for ^{1}H NMR. Assignments are based on the proposed molecular structure. Comparative NMR data from Rodrigues et al. (2014) are provided for reference. *Abbreviations:* s = singlet; d = doublet; dd = doublet of doublets; t = triplet; m = multiplet; J = coupling constant (Hz); δ = chemical shift (ppm)

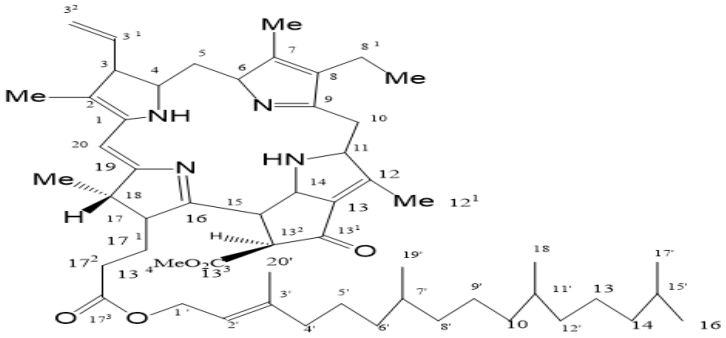

Figure 1: Structure of pheophytin A

Characterization of MPH-29 as stigmasterol

This fraction was obtained as a white crystalline solid from the ethyl acetate fraction. The HR–LCMS detected a dominant molecular ion at m/z 413.3734 corresponding to the protonated molecular ion $[M + H]^+$ species of a neutral molecule with an exact molecular mass of 412.3705 Da and the molecular formula C29H48O consistent with stigmasterol

Table 2 revealed several signals. Oxymethine proton at 3.52 (1H, tdd, J = 11.1 Hz, H-3). A set of tertiary and secondary methyl groups was observed between 0.67-1.52 ppm, including two singlets at 1.00 and 0.72 attributable to Me-19 and Me-18, and four doublets at 0.92 (Me-21), 0.85 (Me-26), 0.83 (Me-29), and 0.81 (Me-27). Other data are three vinylic protons at δ 5.11, 5.41, and 5.54. The δ 5.54 ppm is the proton (H-6) at carbon 6 of the double bond between C5-C6. This proton is relatively deshielded because it sits in the rigid steroid ring system and is influenced by the 3β-OH and ring currents, so it often appears downfield ~5.3–5.6 ppm. (Sai *et al*., 2012). The other two vinylic protons are the H-22 and H-23 associated with the double bond at C-20 and C-21, respectively.

The ^{13}C NMR data in Table 2 showed olefinic carbon at 140.76, 138.36, 129.6, 121.76 ppm, and one oxygenated methine at 71.83 ppm, which is a classical fingerprint of stigmasterol.

2D NMR (HSQC, COSY and HMBC) were observed for connectivity. The HSQC data revealed a correlation between C-6 at 121.76 ppm and H-6 at 5.54 ppm, C-20 at 129.26 and H-20 at 5.41 ppm, C-21 at 138.36 ppm and H-21 at 5.11 ppm. The oxymethine C-3 at 71.83 is linked to H-3 at 3.52.

COSY correlation revealed a cross peak between H-20 and H-21 trans side-chain alkene, an allylic connection between H-6 and H-7, and H-3 to H-2. The 1D and 2D NMR data from this study were compared with relevant literatures, (Sai *et al*., 2012), (Shwe *et al*., 2019) and used to assign structure to this compound (Figure 2)

Antimicrobial activity of the isolated compounds

The antimicrobial activities of two isolated compounds, MPH-12 (pheophytin A) and MPH-29 (stigmasterol), were evaluated against *Salmonella gallinarum* and *Salmonella pullorum*. The study utilized Agar well diffusion analysis to determine the compounds' efficacy, revealing that both exhibited significant antibacterial activity. At a concentration of 100 µg/mL, MPH-12 produced the largest zone of inhibition (23 mm), indicating a stronger antibacterial effect compared to MPH-29. Notably, both compounds demonstrated concentration-dependent responses, with larger inhibition zones occurring at higher concentrations, confirming their intrinsic antibacterial potential.

The minimum inhibitory concentration (MIC) was found to be 25 µg/mL for both compounds, in Table 3 effectively preventing visible growth of the tested bacteria. Additionally, the minimum bactericidal concentration (MBC) result in Table 4 revealed that MBC of MPH-12 is 25 µg/mL *S. gallinarum* while that of MPH-29 is 100 µg/mL for *S. pullorum*.

Table 2: NMR experimental data for MPH 29

Position	δ [1] ppm	δ(^{13}C)	(ppm)	Literature Sai *et al*., 2012
C-1	1.07 (m)	37.26		37.60
C-2	1.85 (m)	32.44		32.10
C-3	3.51 (tdd)	71.83	3.53 (tdd, 1H, *J*=4.5, 4.2, 3.8Hz)	72.10
C-4		42.33		42.40
C-5	5.41(t, 1H, J=6.1 Hz	140.76	5.31(t, 1H, J=6.1 Hz)	141.10
C-6		121.76		121.80
C-7		31.90		31.80
C-8		31.90		31.80
C-9		50.15		50.20
C-10		36.52		36.60
C-11		21.13		21.50
C-12		39.78		39.90
C-13		42.33		42.40
C-14		56.87		56.80
C-15		24.38		24.40
C-16		29.13		29.30
C-17		56.09		56.20
C-18		40.54		40.60
C-19	1.00	21.24	0.91 (d, 3H, J= 6.2 Hz)	24.40
C-20	5.11	138.36	4.98 (m, 1H)	138.70
C-21	5.36	129.26	5.14 (m, 1H)	129.26
C-22	0.83	45.82	0.83 (t, 3H, J=7.1 Hz)	46.10
C-23		25.44		25.40
C-24		12.00		12.10
C-25		29.13		29.60
C-26	0.83	20.24	0.82 (d, 3H, J=6.6 Hz)	20.20
C-27	0.82	19.85	0.80 (d, 3H J=6.6)	19.60
C-28	0.72	18.80	0.71 (s, 3H,)	18.90
C-29	1.07	12.29	1.03 (s, 3H)	12.20

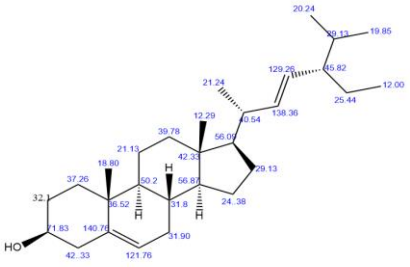

Figure 2: Structure of stigmasterol

Table 3: Antimicrobial activity of the isolated compounds

Concentrations(µ)	Tested organism	Zone of inhibition(mm)	
		MPH-12	MPH-29
100	*S. pullorum*	23	22
	S. gallinarum	15	15
50	*S. pullorum*	19	19
	S. gallinarum	13	12
25	*S. pullorum*	17	10
	S. gallinarum	10	10

Antibacterial activity of MPH-12 and MPH-29 against *Salmonella pullorum* and *Salmonella gallinarum* at different concentrations, expressed as zones of inhibition (mm). *Abbreviations:* mm = millimeters; µ = microgram (µ).

Table 4: Minimum Inhibition Concentration (MIC) and Minimum Bactericidal Concentrations (MBC) of the isolated compounds

Concentrations(µg/mL)	Tested organism	MIC		MBC	MBC
		MPH-12	MPH-29	MPH-12	MPH-29
100	*S. pullorum*	-	-	50	100
	S. gallinarum	-	-	25	25
50	*S. pullorum*	-	-		
	S. gallinarum	-	-		
25	*S. pullorum*	-	-		
	S. gallinarum	-	-		

Keys: (-) means no growth at these concentrations

.

In silico result of isolated compounds

Docking analysis revealed that stigmasterol binds within a defined binding pocket of the OmpC protein in both *S. gallinarum* Figure 3 and *S. pullorum* Figure 4. The predicted binding affinities were −3.886 kcal/mol for *S. gallinarum* and −4.493 kcal/mol for *S. pullorum*. The examination of interaction maps for stigmasterol in the OmpC binding pocket of *S. pullorum* and *S. gallinarum* revealed that it predominantly occupies a hydrophobic region, with its steroidal backbone engaging in nonpolar contacts with hydrophobic amino acids in the protein. In *S. pullorum*, the hydroxyl (–OH) group of stigmasterol forms a specific interaction with tyrosine (TYR 221), which is structurally linked to glycine (GLY 219), while in *S. gallinarum*, the –OH

group interacts with cysteine (CYS 317) linked to histidine (HIS 318)

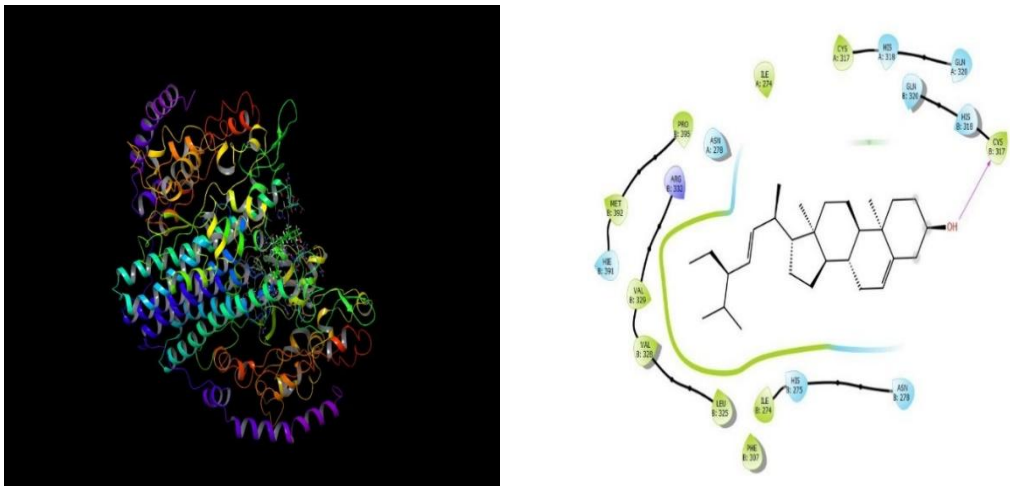

Figure 3: 3D and 2D interaction of the outer membrane C of *S. gallinarum* with stigmasterol

In contrast, pheophytin A could not be successfully docked due to its high molecular weight and bulky structure, suggesting alternative mechanisms of action for its antimicrobial activity

ADMET predictions of the isolated compounds

The ADMET profiles (Table 5) of the isolated compounds, pheophytin A and stigmasterol, were evaluated using in silico prediction tools. Pheophytin A has a consensus log P value of 9.9, while stigmasterol has a value of 6.96, indicating high lipophilicity, with pheophytin A being more lipophilic. Pheophytin A is insoluble in water, whereas stigmasterol is moderately soluble, which may affect their movement in the blood. In terms of oral drug-likeness, pheophytin A violates 2 of Lipinski's rules, while stigmasterol violates 1, making stigmasterol the more suitable candidate. Stigmasterol's bioavailability is 55% compared to 17% for pheophytin A, with a minimum requirement of 50% for effective administration (Demian *et al*., 2024). Both compounds showed low gastrointestinal absorption, with pheophytin A binding to the P-gp substrate and stigmasterol to the CYP2C9 inhibitor, while other parameters related to pharmacokinetics remained unaffected

Toxicity profile

Protox 3 was used to predict the toxicity of the isolated compounds, as shown in Table 6, revealing that stigmasterol has an LD_{50} of 890 mg/kg and pheophytin A has an LD_{50} of 40 mg/kg. For acute oral toxicity class, stigmasterol and pheophytin A are classified as class 4 and 2 respectively. There was no hepatotoxicity, carcinogenicity, mutagenicity, or cytotoxicity.

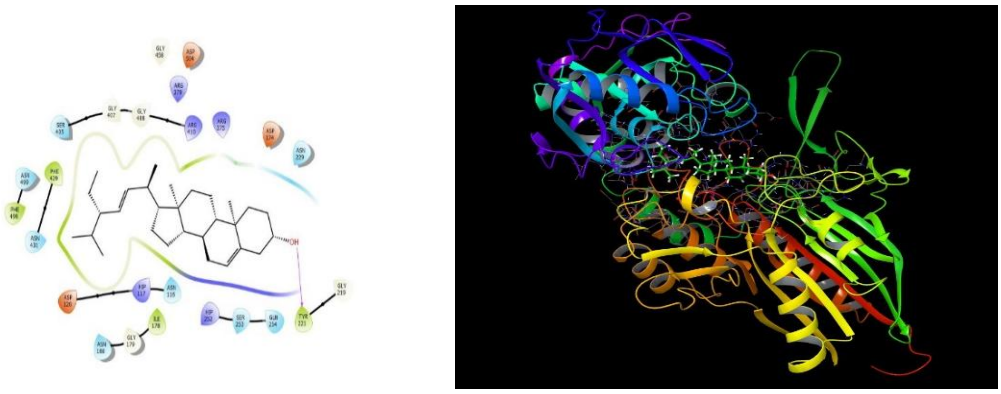

Figure 4: 3D and 2D interaction of the outer membrane C of *S. pullorum* with stigmasterol ADMET predictions of the isolated compounds

Table 5: ADMET results of the isolated compounds

COMPOUNDS	iLOGP	XLOGP3	WLOGP	MLOGP	silicos-IT class	Consensus log P	Classof solubility(water)	bioavailability	drug likeness
Pheophytin A	7.24	11.72	11.43	4.96	14.19	9.9	insoluble	0.17	2 violation
Stigmasterol	5.08	8.56	7.80	6.62	6.86	6.96	Moderately soluble	0.55	1 violation

Table 6: Protox 3 toxicity profile

Toxicity profile	Pheophytin A	Stigmasterol
Predicted LD_{50}	40 mg/kg	890 mg/kg
Acute oral toxicity class	2	4
Hepatoxicity	Inactive	Inactive
Carcinogenicity	Inactive	Inactive
Immunotoxicity	Inactive	Inactive
Mutagenicity	Inactive	Inactive
Cytotoxicity	Inactive	Inactive

Discussion

The isolated compounds were characterized and identified with mass spectra and NMR data. Comparing the data with published literatures helped to confirm that the MPH-12 is pheophytin A and MPH-29 is stigmasterol.

Overall, the antimicrobial evaluation demonstrated that the isolated compounds MPH-12 (pheophytin A) and MPH-29 (stigmasterol) possess significant antibacterial activity against *Salmonella gallinarum* and *Salmonella pullorum*. The concentration-dependent inhibition, measurable zones of inhibition, defined MIC and MBC values, and antibacterial effects collectively highlight the significance of this work. These findings confirm that the isolated phytochemicals are responsible for the antibacterial activity of the plant and support their potential relevance, which can be used in the control of fowl typhoid and pullorum disease, which are of veterinary importance.

In this study, *in silico* molecular docking was employed to investigate the interaction of stigmasterol with the outer membrane protein C (OmpC) of *Salmonella gallinarum* and *Salmonella pullorum*, to provide molecular-level insight into its observed anti-*Salmonella* activity. OmpC is a trimeric porin protein embedded in the outer membrane of Gram-negative bacteria and is involved in passive diffusion of small molecules, maintenance of membrane integrity, and bacterial virulence (Arnaud *et al*., 2006). Consequently, it represents a biologically relevant target for antimicrobial intervention. The *in silico* molecular predicted binding affinities −3.886 kcal/mol for *S. gallinarum* and −4.493 kcal/mol for *S. pullorum*, indicated a spontaneous and thermodynamically favorable interaction. The more negative binding energy observed with *S. pullorum* suggests a stronger and more stable ligand–protein complex, which may partly explain differences in susceptibility between the two pathogens. The interaction of *S. pullorum* and the hydroxyl (–OH) group of stigmasterol forms a specific interaction with tyrosine (TYR 221), which is structurally linked to glycine (GLY 219), while in *S. gallinarum*, the –OH group interacts with cysteine (CYS 317) linked to histidine (HIS 318). These interactions are significant due to the presence of aliphatic and aromatic amino acids that promote strong van der Waals and hydrophobic interactions, essential in membrane proteins.

Stigmasterol's rigid tetracyclic steroid nucleus and hydrophobic alkyl side chain enhance its affinity for membrane-associated proteins, with the hydroxyl group stabilizing its binding within OmpC. This binding may disrupt porin-mediated transport, impair nutrient uptake, and increase bacterial susceptibility to stress, ultimately hindering bacterial growth. (Pagadala *et al*., 2017) . The compound's targeted interaction with outer membrane proteins suggests a mechanism for its antibacterial effects against Salmonella species, compromising their first line of defense.

Differences in binding affinity between the two bacteria may be due to variations in amino acid composition in the OmpC binding pocket, affecting hydrogen bond strength and complex stability. Such strain-specific differences in porin-ligand interactions have been noted in other studies. (Padikkamannil *et al*,. 2021).

The poor aqueous solubility of pheophytin A, is primarily due to its long hydrophobic phytyl ester chain (C_{20}) attached to the chlorin macrocycle. This aliphatic chain greatly increases lipophilicity (high log P), reduces polarity, and limits interaction with aqueous media, which in turn affects bioavailability and pharmacokinetics. This phytyl group is the primary contributor to excessive lipophilicity (very high log P), poor aqueous solubility, and low predicted oral bioavailability. Because the phytyl chain is attached via an ester linkage, it represents a chemically accessible site for structural modification.

To improve the drug-likeness of pheophytin A, the phytyl chain can be removed by dephytylation and subsequent replacement by re-esterification with short-chain alkyl esters or hydroxyl-containing alcohol or amide formation, in which the carboxyl group is converted into amide linkages. This modification or optimization often improves oral drug-likeness, introduces substituents capable of partial ionization, improves dissolution in physiological pH, and reduces excessive membrane binding (Demian *et al*., 2024) . Replacing the phytyl chain with smaller or more polar substituents directly addresses the major ADMET limitations observed for pheophytin A (Thomas and Donald, 2005)

The toxicity profile revealed a clear difference in the acute toxicity levels of pheophytin A and stigmasterol, while both compounds exhibit similarly favorable safety characteristics across other toxicity endpoints.

Pheophytin A is significantly more toxic than stigmasterol, with predicted LD_{50} values of 40 mg/kg and 890 mg/kg, respectively. This indicates that a lower dose of pheophytin A can produce toxic effects, classifying it as Class 2 for acute oral toxicity, while stigmasterol is Class 4, reflecting its lower toxicity. However, both compounds show inactive profiles in other toxicity parameters such as hepatotoxicity, carcinogenicity, immunotoxicity, mutagenicity, and cytotoxicity, suggesting they do not pose risks for these conditions. Overall, while pheophytin A has higher acute toxicity, both compounds are considered to have favorable safety profiles for potential pharmacological applications, provided dosage considerations are taken into account, especially for pheophytin A.

Conclusion

Structural elucidation using Nuclear Magnetic Resonance spectroscopy and Mass Spectrometry confirmed the identities of the isolated compounds to be pheophytin A and stigmasterol. The two compounds demonstrated antimicrobial potential against *Salmonella gallinarum* and *Salmonella* with pheophytin A showing superior activity.

Furthermore, integration of in vitro antimicrobial data with in silico ADMET and drug-likeness analyses provided preliminary insight into the pharmacokinetic behavior and safety profiles of the isolated compounds, supporting their potential as lead molecules for antimicrobial drug development. Overall, this study advances the phytochemical and pharmacological knowledge of *Senna siamea*, highlights pheophytin A as a promising anti-Salmonella agent, and provides a scientific foundation for the development of plant-derived alternatives to conventional antibiotics in poultry disease management.

Conflict of Interest

The authors declare no conflict of interest

Authors' Declaration

The authors hereby declare that the work presented in this article is original and that any liability for claims relating to the content of this article will be borne by them.

Acknowledgements

The authors are grateful to the National Veterinary Research Institute, Vom, for enabling a laboratory environment for the success of this study, and Mr. Mark Audu of FCMLT Vom for his assistance during the molecular docking, and to all staff in the Microbiology Lab, Central Diagnostics, NVRI Vom, for their assistance.

References

Abdulrasheed M, Hussein I, Siddan, IA (2015). Determining the Phytochemical Constituents and the Antimicrobial Activity of Ethanolic Extract of Acassia Leaf (*Senna siamea*) on Some :Enterobacteriaceae. *IOSR Journal Of Pharmacy 5*(6), 18–22. www.iosrphr.org

Arnaud B, Gabriele R, Paola S, *et al* (2006). Crystal Structure of Osmoporin OmpC. *Journal of Molecular Biology* 362: 933–942. https://doi.org/10.1016/j.jmb.2006.08.002

Berhanu G, Fulasa A (2020). Pullorum Disease and Fowl Typhoid in Poultry: A Review. *British Journal of Poultry Science 9*(3): https://doi.org/10.5829/idosi.bjps.2020.

Demian DM, Amasiorah IV, Johnson OT *et al* (2024). Phytochemical identification and in silico elucidation of interactions of bioactive compounds from *Citrullus lanatus* with androgen receptor towards prostate cancer treatment. *In Silico Pharmacology 12*(27): 1-14. https://doi.org/10.1007/s40203-024-00193-5

FAO (2016). *The FAO Action Plan on Antimicrobial Resistance* 2016-2020, 1-13.

Friday C, Igwe OU, Clinton AU. (2021). NMR characterization and free radical scavenging activity of pheophytin 'A' from the leaves of *Dissotis rotunifolia*. *Bulletin of Chemical Society Ethiopia 35*(1): 207–215. https://doi.org/dx.doi.org/10.4314/bcse.v35i1.18

Lisa Nichols. (2021). *OChem LabTechniques*. Organic Chemistry Laboratory Techniques. https://www.coursehero.com/file/80820362/OChem-LabTechniques-2ndEdpdf/

Marangoni F, Corsello G, Cricelli C *et al,* (2015). Role of poultry meat in a balanced diet aimed at maintaining health and wellbeing: an Italian consensus document. *Food and Nutrition Research 59:* 1–11. https://doi.org/10.3402/FNR.V59.27606

Nas FS, Oyeyi TI, A. M. (2018). Antibacterial efficacy and phytochemical screening of *Senna siamea* leaves extracts on some pathogenic bacteria. *Journal of Microbiology and Experimentation 6*(3): 159-163. https://doi.org/10.15406/JMEN.2018.06.00208

Nützmann HW, Huang A, Osbourn A (2016). Plant metabolic clusters – from genetics to genomics. *New Phytologist* 211(3): 771–789. https://doi.org/10.1111/NPH.13981

Odo, P, Ngozi A, Ekene O, Chiaguguom I, Grace, F. (2022). Isolation of Pheophytin A and β -amyrin from *Newbouldia laevis* (P . Beauv) Leaf Extract. *Path of Science 8*(6): 7001–7012. https://doi.org/10.22178/pos.82-16

Otor EM, Akpomie T, Usman A (2025). Effect of Different Extracts and Fractions of *Senna Siamea* Leaf on *Salmonella gallinarum* and *Salmonella pullorum*. *Tropical Journal of Phytochemistry and Pharmaceutical Sciences 4*(9): 378–383. https://doi.org/www.doi.org/10.26538/tjpps/v4i9.1

Padikkamannil A, Pollumahanti N, Varsha U *et al*., (2021). In silico molecular docking and antimicrobial efficacy of phytochemicals against multi-drug-resistant enteroaggregative *Escherichia coli* and non-typhoidal Salmonella spp. *Gut Pathogens 13(1):46* https://doi.org/https://doi.org/10.1186/s13099-021-00443-3

Pagadala NS, Syed K, Tuszynski J (2017). Software for molecular docking : A review. *Biophysical Reviews* 9(2): 92-102. https://doi.org/10.1007/s12551-016-0247-1

Rodrigues GC, Isla VG, Jose AS *et al*, (2014). Free radical-scavenging activity and cytotoxicity from leaves of *Guettarda*

platypoda. *Issues in Biological Sciences and Pharmaceutical Research 2*(9): 99-105. https://doi.org/dx.doi.org/10.15739/ibspr.003

Sai V, Chaturvedula P, Prakash I (2012). Isolation of Stigmasterol and β -Sitosterol from the dichloromethane extract of *Rubus suavissimus*. *International Current Pharmaceutical Journa 1*(9): 239–242.

Shivaprasad HL (2000). Fowl typhoid and pullorum disease. *Revue Scientifique et Technique (International Office of Epizootics* 19(2): 405–424. https://doi.org/10.20506/RST.19.2.1222

Shrivastava R, Mishra J (2019). Extraction, Phytochemical Screening, Isolation and Identification of Bioactive Compounds from Extract of the plant *Euphorbia thymifolia Linn*. *Journal of Drug Delivery and Therapeutics 9*(3): 107–113. https://doi.org/10.22270/JDDT.V9I3.2608

Shwe HH, Thein WW, Win SS *et al*, (2019). Structural Characterization of Stigmasterol and β - Sitosterol from the Roots of *Premna herbacea* Roxb. *International European Extended Enablement in Science, Engineering and Mnagement 7*(8): 195–201.

Thomas N, Donald FW (2005). Medicinal Chemistry: A molecular and biochemical approach. 3rd Ed. 9-43

Zhou, X., Kang, X., Zhou, K., & Yue, M. (2022). A global dataset for prevalence of *Salmonella gallinarum* between 1945 and 2021. *Scientific Data 9*(1): 1–11. https://doi.org/10.1038/s41597-022-01605-x

Ziaul HAKM, Akter MR, Islam SKS, *et al*, (2021). *Salmonella gallinarum* in small-scale commercial layer flocks: Occurrence, molecular diversity and antibiogram. *Veterinary Sciences 8*(5): 1-16. https://doi.org/10.3390/vetsci8050071

CITATION Otor ME, Akpomie T Usman A (2026) Isolation and Characterization of Bioactive Compounds in S*enna siamea* Leaf and their Inhibitory Activity Against *Salmonella gallinarum* and *Salmonella pullorum.* Trend Nat Prod Res Vol 7 (3):239-251. https://doi.org/10.61594/tnpr.v7i3.2026.171